Methodology for the optimal thermo-economic, multi-objective design of thermochemical fuel production from biomass

Martin Gassner, François Maréchal

Laboratory for Industrial Energy Systems
Ecole Polytechnique Fédérale de Lausanne
CH – 1015 Lausanne, Switzerland

Computers and Chemical Engineering 33 (2009) 769-781, doi:10.1016/j.compchemeng.2008.09.017

Abstract

This paper addresses a methodology for the optimal conceptual design of thermochemical fuel production processes from biomass. A decomposed modelling approach with separate energy-flow, energy-integration and economic models are coupled with a multi-objective optimisation strategy. It is applied to the design of a process that produces synthetic natural gas (SNG) from lignocellulosic materials. The systematic choice of the objectives thereby assures the generation of a general set of optimal process flowsheets, which constitute a sound basis for the synthesis of a viable plant. Statistical methods are used to realise a detailed multi-criteria analysis of the results.

Keywords: biofuels, bioenergy, gasification, methanation, electrolysis, optimisation, SNG

Nomenclature

Abbreviations

FT	Fischer Tropsch
$HE(N)$	Heat exchanger (network)
MER	Minimum energy requirement
$MI(N)LP$	Mixed integer (non-)linear programming
$(S)NG$	(Synthetic) natural gas

Roman letters

A	Heat exchanger area	m^2
b_{HE}	Cost exponent for heat exchangers	-
c_1	Cost factor to account for contingencies and fees	-
c_2	Cost factor to account for site development and auxiliary facilities	-
C_{BM}	Bare module cost	€
C^0_{BM}	Bare module cost at base case conditions	€
C_{el}	Electricity price	€/MWh
C_{GR}	Grass roots cost	€
C_M	Maintenance costs	€/MWh
C_{OL}	Operating labour costs	€/MWh
C_{OP}	Operating costs	€/MWh
C_P	Total production costs	€/MWh
C_{RM}	Raw material costs	€/MWh
$C_{salaries}$	Employees salaries	€/year
C_{UT}	Utility costs	€/MWh
C_{wood}	Wood price	€/MWh

$\dot{E}_q$	Mechanical power potential of heat	kW
$\dot{e}_{q,s}$	Specific mechanical power potential of heat from subsystem s	kW
$e_{a,i}$	Specific avoided CO_2 emissions assigned to substance i	kg/MWh$_i$
$e_{p,i}$	Specific CO_2 emissions assigned to the production of substance i	kg/MWh$_i$
e_{plant}	Specific CO_2 emissions from plant	kg/MWh$_{wood}$
f_s	Multiplication factor accounting for extensive variables of subsystem s	-
i_r	Interest rate	%
$\dot{L}$	Exergy depletion	kW
$\dot{m}$	Mass flow	kg/s
n	Expected plant lifetime	years
P_a	Yearly production	MWh/year
p_a	Adsorption pressure	bar
p_g	Gasification pressure	bar
p_m	Methanation pressure	bar
$p_{s,p}$	Steam production pressure	bar
$\dot{Q}$	Heat	kW
$\dot{q}_s$	Specific production of heat by subsystem s	kW
$\dot{R}_r$	Cascaded energy from temperature interval $r+1$ to r	kW
$r_{S/B}$	Steam to dry biomass ratio	%wt
$T_{d,in}$	Drying temperature at inlet	K
$T_{g,p}$	Preheat temperature of gasification agent	K
T_g	Gasification temperature	K
$T_{m,in}$	Methanation temperature at inlet	K
$T_{m,out}$	Methanation temperature at outlet	K
$T_{s,c}$	Steam condensation temperature	K
$T_{s,s}$	Steam superheat temperature	K
$T_{s,ui}$	Temperature of utilisation level i	K
$\dot{W}$	Electrical power	kW
$\dot{w}$	Specific electrical power of subsystem s	kW
y_s	Integer variable representing the presence of subsystem s	-
Greek letters		
α	Convective heat transfer coefficient	kW/(m^{2}K)
Δh_i	Lower heating value of substance i	MJ/kg
ΔH_r	Heat of reaction	kJ/mol
Δh_{vap}	Latent heat of vaporisation	MJ/kg
Δk_i	Exergy value of substance i	MJ/kg
ΔT_{lm}	Logarithmic mean temperature difference	K
ΔT_{min}	Minimum approach temperature	K
ΔT_{ref}	Reference approach temperature	K
ε	Energy efficiency	%
η	Exergy efficiency	%
μ	Mean value	
$\Phi_{w,out}$	Wood humidity after drying	%wt
Φ_w	Wood humidity at process inlet	%wt
ρ	Correlation coefficient	-
σ	Standard deviation	
Superscripts		
$*$	Corrected temperatures	
$+$	Material or energy stream entering the system	
$-$	Material or energy stream leaving the system	
0	Standard or base case conditions	

1 Introduction

Thermochemical processes for the production of fuels from renewable resources are highly integrated energy conversion systems. In addition to the technology development, the performances of such processes relies on the quality of the design and mainly on the quality of the process integration. Most of the thermo-economic process investigations addressing the production of Fischer Tropsch (FT) liquids, Synthetic Natural Gas (SNG) and the coproduction of these fuels are based on conventional simulation of some flowsheet scenarios developed by engineers' intuition and knowledge (Tijmensen et al., 2002; Hamelinck et al., 2004; Mozaffarian and Zwart, 2003; Zwart and Boerrigter, 2005). Considering the large number of design options resulting from the choice of the available technologies and the process integration options, a systematic process design method appears to be necessary. The uncertain nature of the design parameters thereby suggests an approach using multi-objective optimisation in order to capture relationships between conflictive objectives. From engineering perspectives, understanding the links between decision variables and objective functions is also an issue.

Systematic methodologies for preliminary process design based on process integration techniques and multi-objective optimisation have already been developed and applied to power plants and solid oxide fuel cell systems design (Bolliger et al., 2005; Palazzi et al., 2005). In the field of biofuel production, such computer aided process synthesis methodologies have not really been applied. The present paper aims at presenting the developed process design methodology for the conceptual design of thermochemical biofuel production processes and demonstrate its application to the production of SNG from wood.

2 Design methodology

The basic concept of the developed method is the decomposition of the problem into several parts, as illustrated in Figure 1. Following the conceptual process design methodology (Douglas, 1985), the block flow diagram of the conversion process is first set up. After identifying suitable technology for the conversion steps, energy-flow, energy-integration and economic models of the equipment and their interactions are integrated in a multi-objective optimisation framework to compute a set of optimal process configurations with respect to different design objectives. An analysis of the optimisation results with regard to environomic (i.e. thermodynamic, economic and environmental) criteria then results in the synthesis of sound conceptual plant flowsheets.

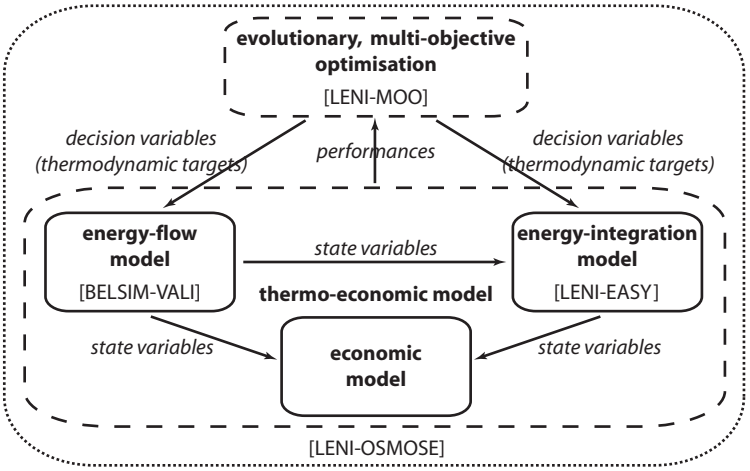

Figure 1: Design methodology overview.

2.1 Block flow superstructure

In the first step of the design, the product specifications and the available raw materials and energy resources are investigated and the general requirements on the process are defined. This determines feasible production pathways, required process steps and intermediate products. For the block flow diagram, suitable technologies and mandatory auxiliary operations such as feed preparation, product purification and recycling are identified and assembled in a process superstructure. The components of the heat recovery system and optional additional equipment for optimal energy conversion complete the superstructure. The definition of possible material pathways and the identification of the range of operating conditions for which the transformations are thermodynamically and technically feasible concludes the technology identification step and results in the definition of the design problem.

2.2 Flowsheet generation by thermo-economic modelling

After the definition of the block flow superstructure, there exist several ways of formulating and solving the problem of generating feasible process configurations (flowsheets). Such formulations are influenced by the chosen optimisation algorithm for the subsequent optimisation step. Considering the number of options in the process superstructure, the explicit description of the heat exchanger network (HEN) appears a priori too complex due to the combinatorial nature of the problem and the large number of possible options. One alternative is the use of a generalised heat exchanger network superstructure as proposed by Floudas et al. (1986). This however defines a very complex mixed integer non-linear programming (MINLP) problem since the heat exchanger network superstructure has to be combined with the process superstructure, in which the choice of the process options and its operating conditions have to be optimised together with the utility system and the heat exchanger network design. Alternatively, the use of the heat cascade constraints allow for modelling the performances of the HEN. Unlike conventional flowsheeting methods, this approach does not define the topology of the heat exchanger network and the fuel supply a priori, but computes it in the integration step. No restrictions are thus set on the system design and a maximum number of potential solutions are considered, which makes the method very suitable for conceptual process design. When using pinch analysis for modelling the HEN, a classical sequential approach as proposed by Douglas (1988) can be used to solve the design problem: first the energy flows are modelled using a flowsheeting approach, then the pinch analysis is used to compute the maximum heat recovery by heat exchange and finally the heat exchanger network is designed. If in our approach, the principle of this approach is applied, the method proposed had however to be adapted in order to overcome some of the weaknesses of the classical sequential approach. In conventional pinch analysis, only the minimum energy requirements are considered and the utility streams used to close the energy balance are considered at a given temperature (supposed to be sufficient). Furthermore, the pinch analysis does not include the combined heat and power production and the cost of the heat exchanger network is difficult to estimate since the utility streams are not considered. In order to solve the problem, a formulation as proposed by Kravanja and Glavic (1997) has been investigated to overcome such weaknesses. This approach first divides the optimisation problem into several successive mathematical programming steps. A decomposition strategy is used to partition the decision variables that affect the performances of the process flowsheet, and the problem is solved in a discretised space. The process integration and HEN targeting problem is solved as a MINLP problem. Using the results of this mathematical programming approach, a detailed model for solving and optimising the HEN design using a NLP problem is then applied. One of the major contributions of this method is the heat integration and HEN cost targeting method that is solved simultaneously with the flowsheeting aspects. Regarding the typical problem to be solved in thermochemical biomass to fuel conversion, there are however still some unsolved problems. The first one is related to the utility system. In the case of Kravanja and Glavic, the utilities are considered as external streams. In our case, there are no utility streams since the raw material (biomass), the product (SNG), the intermediate streams and even some of the waste streams are all able to produce the required heat for the conversion process. The heat requirement will therefore be satisfied by selecting the appropriate flows in the conversion process itself and the quality of the integration will

define the efficiency of the process. The second difficulty relates to the process flowsheet superstructure. As different technologies may be used to realise the identified process operations, the process flowsheet is in reality a complex superstructure including a lot of different options that will be selected for their role in the production and/or in the energy integration. As the operating conditions have to be optimised together with the existence of only some of the technologies in the final design, this would require the application of disjunctive programming techniques. The third difficulty is the combined heat and power (CHP) production that is used in order to valorise the exergy of the streams. The quality of the process integration therefore depends on the simultaneous optimisation of the mechanical power balance and the heat integration. As steam will be used for CHP, the pressure levels have to be optimised. This would create problems in a mathematical programming formulation due to the non-continuous nature of the heat cascade when the temperature of the streams is changing. Finally, in addition to the HEN costing, the cost estimation technique for the process implies the sizing of the different technologies based on their expected operating conditions. As such sizing procedures may be discontinuous due to the application of if-then-else rules or limits of elements, this would require the use of integer variables and special constraints if one would formulate the problem as a mathematical programming problem. In addition, our goal was to use a multi-objective optimisation strategy in order to understand the trade-off between conflicting objectives and to define sets of configurations. From the mathematical programming perspective, this would require the use of integer cuts and the application of parametric programming and therefore the resolution of a large number of MINLP problems.

We have therefore reformulated the problem in order to resolve these drawbacks. The proposed method is based on the following principles:

1. The decision variables set is decomposed into two subsets: (a) the complicating variables that are handled by an evolutionary algorithm that solves a multi-objective optimisation problem and (b) the superstructure variables that are selected such that they allow to formulate the process integration model as a MILP problem. The complicating variables define the operating conditions of the different technologies. Using the flowsheeting model, these variable determine the hot and cold streams to be considered in the heat cascade as well as the mass balances from the superstructure.

2. The flowsheeting model uses an equation solver procedure and the complicating decision variables are set as specifications for the flowsheeting problem. They are selected to guarantee the convergence of the flowsheeting problem.

3. The superstructure model is formulated as a mixed integer linear programming (MILP) model that includes the heat cascade, the combined heat and power production and the mass balance of the technology superstructure. The objective function of this problem is the operating cost of the system.

4. The reference approach temperature ΔT_{ref} is considered as a complicating decision variable and is used to represent the energy recovery/capital trade-off in the HEN design. It will be used as the sizing decision variable for targeting the HEN cost.

5. The cost of the HEN is estimated considering the composite curves as computed by the process integration model and the minimum number of units as obtained from the graph theory.

6. The different equipment is sized independently as a function of the operating conditions imposed by the set of complicating variables and the flows as computed in the process integration model. Their cost is then deduced from the size and not from capacity-based correlations.

7. The model is solved in three successive steps: the flowsheeting step, the process integration step and the sizing and costing step. The objective functions are calculated at the end of these three steps.

8. An evolutionary multi-objective optimiser is used to optimise the value of the complicating decision variables.

9. The set of complicating decision variables is defined such that the inequality constraints will appear either as bounds on the decision variables or as linear inequality constraints in the process integration model and therefore will be handled by the MILP algorithm.

10. The mathematical formulation of the process unit models are not available as a set of explicit equations and may be computed using different flowsheeting software.

11. The final design of the heat exchanger network will be defined after the process optimisation procedure and only for a limited number of optimal process configurations from the Pareto curves. It is assumed that the HEN design can be solved using conventional HEN design routines and that the optimal design will feature investment and operating cost that will be close to the one estimated by the composite curve model.

According to these principles, the thermodynamic conditions of the process unit operations are first calculated in the energy-flow model. The energy conversion and heat transfer system is then calculated in the energy-integration model using heat cascade constraints and a combined heat and power maximisation method, as explained in detail below.

2.2.1 Energy-flow model

The goal of the energy-flow model is to compute the material conversion in the process units, to determine their heat transfer and power requirements and to thermodynamically characterise the streams that will be used for the equipment rating. Such thermodynamic transformation models are developed for all process equipments of the block flow superstructure. In addition to the mass and energy balances and the thermochemical conversion of the species, the thermodynamic unit models also define the power requirements and the enthalpy-temperature profiles that represents the heat transfer requirement. The energy-flow models are developed using the commercial flowsheeting tool *Belsim-Vali*, (Belsim SA, 2007), which is based on an equation solver formulation that does not require the definition of a resolution sequence. This eases the handling of problems with stream loops and further allows for model reconciliation with experiment and pilot plant data.

2.2.2 Energy-integration model

Once the heat and power requirements of the transformations defined, the heat cascade is used to model the heat exchanger network. Flows in the system are optimised in order to maximise the combined heat and power production in the plant. The thermal effects of each sequence of operations without stream bifurcation are grouped and constitute the units whose flowrates are to be computed in the integration problem. In order to supply the energy requirement above the pinch, combustion of fuels available on-site is considered. Dissociating the effects of the fuel and combustion air as outlined by Maréchal and Kalitventzeff (1998), the thermal effects of the usable waste and retentate streams are formulated. If the heat available from their combustion is not sufficient, process streams may be used as fuel to close the balance leading to a reduction of the flows in the main conversion route. The choice of using optional energy conversion and recovery equipment like heat pumps, gas turbines and Rankine cycles is formulated by means of integer variables. The structure and operating conditions of these units are predefined and considered as decision variables of the overall design problem. If a certain technology is considered, only the corresponding flowrates are calculated by the energy-integration model.

The model developed to represent the heat recovery and conversion system is based on a MILP formulation that uses the heat cascade as constraints and assumes a minimum approach temperature ΔT_{min}. In order to account for different values of the heat transfer coefficient, the corrected temperatures T^* that

are used for computing the heat cascade are calculated by Equations 1 and 2:

$$T_h^* = (T - \Delta T_{min}/2)_h \quad \forall h \in \{hot\,streams\} \tag{1}$$

$$T_c^* = (T + \Delta T_{min}/2)_c \quad \forall c \in \{cold\,streams\} \tag{2}$$

A heuristic rule (Eq. 3) is used to estimate the value of $\Delta T_{min}/2$ of a stream j when its convective heat transfer coefficient α_j is known:

$$(\Delta T_{min}/2)_j = \frac{\Delta T_{ref}}{2}\left(\frac{\alpha_{ref}}{\alpha_j}\right)^{b_{HE}} \tag{3}$$

where ΔT_{ref} is the minimum approach temperature for an an arbitrary reference heat transfer coefficient α_{ref} and b_{HE} the exponent used in Equation 16 for estimating the cost of the heat exchangers. The value of ΔT_{ref} can be used in the optimisation procedure to represent the trade-off between the investment cost and the heat recovery and energy conversion efficiency.

Knowing the temperatures, pressure, power and nominal flows of the energy conversion units and the process streams, the optimal flowrate of each of the sub-systems in the superstructure will be computed by solving the MILP problem whose mathematical definition is given by Equations 4 – 11. This method will select the equipment in the superstructure and determine their optimal flowrates in the integrated system. Two variables are therefore associated with any subsystem s. The integer variables y_s represent the presence of the subsystem s in the optimal configuration and f_s represents its level of utilisation respecting the associated lower and upper bounds $fmin_s$ and $fmax_s$ (Eq. 6). Beneath the constraints imposed by the heat cascade (Eq. 7), the overall heat balance (Eq. 8) and the electricity balance (Eqs. 9 and 10), additional constraints imposed by the superstructure are added in the form of a system of linear equations (Eq. 11) to account for the material balances between the subsystems and the production specifications. In order to maximise the combined fuel, heat and power production, the objective function to be minimised is the exergy depletion $\dot{L}$. For all subsystems, it is calculated by balance (Eq. 4) and accounts for the exergy destruction in the unit operations and the exergy losses released to the environment.

$$\min_{\dot{R}_r, y_s, f_s} \sum_{s=1}^{n_s} \dot{L}_s = \sum_{s=1}^{n_s} \left(f_s \cdot \left(\sum_{f=1}^{n_{fuel,s}} \dot{m}_{f,s}\Delta k_f^0 + \dot{w}_s^+ - \sum_{r=1}^{n_r} (\dot{e}_{q,s,r}^-)_{\Delta T_{min}} - \dot{w}_s^- \right) \right) \tag{4}$$

where the terms represent:

$\sum_{f=1}^{n_{fuel,s}} \dot{m}_{f,s}\Delta k_f^0$ the exergy consumed as fuel resources to produce the hot and cold streams of the energy conversion unit s in nominal conditions. $n_{fuel,s}$ represents the total number of fuels, $\dot{m}_{f,s}$ the flowrate of each fuel and Δk_f^0 its exergy value.

$\dot{w}_s^+$ the specific consumption of electricity of the subsystem s

$\sum_{r=1}^{n_r} (\dot{e}_{q,s,r}^-)_{\Delta T_{min}}$ the sum of the heat exergy supplied by the hot and cold streams of the subsystem s in the total number n_r of temperature intervals r in its nominal conditions. $(\dot{e}_{q,s,r}^-)_{\Delta T_{min}}$ is given by Eq. 5. For this calculation, the temperatures used are the corrected temperatures, therefore, $(\dot{e}_{q,s,r}^-)_{\Delta T_{min}}$ includes the exergy destruction due to the stream's contributions $(\Delta T_{min}/2)_s$ to the ΔT_{min} assumption.

$$(\dot{e}_{q,s,r}^-)_{\Delta T_{min}} = \sum_{s=1}^{n_{streams,s}} \dot{q}_{s,r}^-\left(1 - \frac{T_0}{T_{lm,r}^*}\right) \tag{5}$$

with:

$n_{streams,s}$ the number of streams of subsystem s

T_0 reference temperature (ambient)

$T_{lm,r}^*$ the logarithmic mean temperature of interval r

$T_{lm,r}^* = \frac{T_{r+1}^* - T_r^*}{ln(\frac{T_{r+1}^*}{T_r^*})}$ if $T_{r+1}^* \neq T_r^*$ and $T_{lm,r}^* = T_r^*$ otherwise

$\dot{w}_s^-$ the specific production of electricity of the subsystem s

subject to:

1. Existence of subsystem s:

$$fmin_s y_s \leq f_s \leq fmax_s y_s \qquad y_s \in \{0,1\},\ \forall s = 1,...,n_s \quad (6)$$

2. Heat balance of the temperature intervals r:

$$\sum_{s=1}^{n_s} f_s \dot{q}_{s,r}^{-} + \dot{R}_{r+1} - \dot{R}_r = 0 \qquad R_r \geq 0 \ \ \forall r = 1,...,n_r \quad (7)$$

3. Overall heat balance:

$$R_1 = 0,\ R_{n_{r+1}} = 0 \quad (8)$$

4. Electricity consumption:

$$\sum_{s=1}^{n_s} f_s \dot{w}_s^{-} + \varepsilon_d \dot{W}^{+} - \dot{W}_c \geq 0 \qquad \dot{W}^{+} \geq 0 \quad (9)$$

5. Electricity exportation:

$$\sum_{s=1}^{n_s} f_s \dot{w}_s^{-} + \varepsilon_d \dot{W}^{+} - \frac{\dot{W}^{-}}{\varepsilon_g} - \dot{W}_c = 0 \qquad \dot{W}^{+} \geq 0,\ \dot{W}^{-} \geq 0 \quad (10)$$

6. Superstructure model:

$$Af = b \qquad A : (n_s \times n_s),\ f,b : (n_s \times 1) \quad (11)$$

with:

A, b	coefficients of the linear equation system defined by the superstructure
f_s	level of utilisation of subsystem s
$fmax_s$	upper bound of f_s
$fmin_s$	lower bound of f_s
$\dot{L}_s$	exergy depletion in subsystem s
n_r	number of temperature intervals r
n_s	number of subsystems s
$\dot{q}_{s,r}^{-}$	the specific net production of heat of subsystem s in the temperature interval r (negative values represent net consumptions)
$\dot{R}_r$	cascaded energy from the temperature interval $r+1$ to r
$\dot{W}^{+}$	the consumption of electricity from the grid
$\dot{W}_c^{+}$	the auxiliary consumption of electricity on-site
$\dot{W}^{-}$	the production of electricity to the grid
$\dot{w}_s^{-}$	the specific net production of electricity of subsystem s (negative values represent net consumptions)
y_s	integer variable for the presence of subsystem s
ε_d	the conversion efficiency from the grid
ε_g	the conversion efficiency to the grid

By this method, we assume that the heat recovery and conversion system will be modelled by a system in which the pinch points will be activated. In the MILP subproblem, only the maximum exergy recovery is thus targeted for a given value of the efficiency-investment trade-off parameter ΔT_{ef}. The investment in the energy conversion units is disregarded and entirely addressed in the overall flowsheet optimisation.

2.2.3 Equipment sizing and cost estimation

The thermodynamic state of the process streams resulting from the energy-flow and -integration steps are used as equipment design targets. A preliminary sizing and cost estimation procedure has been implemented for each unit to take the direct influence of the design variables on the investment cost into

account. For this purpose, equipment design heuristics mainly from Ulrich (1984) combined with data from existing experimental and pilot plant facilities are used to estimate the size of the major process equipment for a given production scale. According to the costing method of Turton et al. (1998), the bare module costs C_{BM}, defined as the installed cost of a unit considering construction material, operating pressure and indirect costs like freights and engineering expenses, are then determined with correlations from the literature. The total grass roots cost C_{GR} of the plant, i.e. the total investment cost for a new production site excluding land, is estimated by summing up and factoring the bare module costs to account for subsidiary expenses:

$$C_{GR} = (1+c_1)\sum_i C_{BM,i} + c_2 \sum_i C^0_{BM,i} \tag{12}$$

In this equation, c_1 accounts for contingencies and fees during construction and c_2 represents the costs for site development and auxiliary facilities. The latter are supposed to be unaffected by the construction materials and operating pressure and therefore related to the bare module costs C^0_{BM} at base case conditions (i.e. carbon steel construction and ambiant pressure). Typically, c_1 and c_2 amount to 18% and 35% of the bare module costs, respectively.

The capital cost of the heat exchanger network is estimated using the method of Ahmad et al. (1990) by considering the balanced hot and cold composite curves that result from the resolution of Equation 4. The heat exchange is thereby specified as a succession of vertical exchanges between the two composite curves, whereas each vertical section is characterised by two inlet and outlet temperatures and one heat load. Considering all the streams j and their respective heat transfer film coefficient $\alpha_{i,j}$ in the vertical heat exchange section i, and considering that the heat load $\dot{Q}_i$ of the vertical section equals $\sum_{h=1}^{n_{hot\_streams}} \dot{Q}_{h,i}$ and also $\sum_{c=1}^{n_{cold\_streams}} \dot{Q}_{c,i}$, the total area A_i of the vertical section i is obtained by summing the contributions of the streams to the vertical exchange i. The total area $A_{tot,MER}$ necessary to fulfil the minimum energy requirement (MER) is then obtained by summing up the vertical sections i, as shown in Equation 13:

$$\begin{aligned} A_{tot,MER} &= \sum_{i=1}^{n_{vert\,sections}} A_i(\Delta T_{ref}) \\ &= \sum_{i=1}^{n_{vert\,sections}(\Delta T_{ref})} \left(\frac{\dot{Q}_i(\Delta T_{ref})}{\Delta T_{lm,i}(\Delta T_{ref})} \sum_{j=1}^{n_{streams,i}} \frac{1}{\alpha_{i,j}} \right) \end{aligned} \tag{13}$$

The minimum number of exchangers $N_{HE,min,MER}$ to fulfil the target is obtained from the graph theory:

$$N_{HE,min,MER} = (N_s + N_{s,u}(\Delta T_{ref}) - 1) + (N_p(\Delta T_{ref}) - 1) \tag{14}$$

where N_s represents the number of process streams involved in the heat recovery system, $N_{s,u}$ the number of utility streams used to close the energy balance of the system and N_p the number of streams that cross the pinch points and that have to be accounted twice to estimate the number of connections.

It is then possible to estimate the heat exchanger network investment by equally distributing the overall area between the heat exchangers. Therefore, the mean area of one heat exchanger is computed by Equation 15:

$$A_{mean} = A_{mean}(\Delta T_{ref}) = \frac{A_{tot,MER}(\Delta T_{ref})}{N_{HE,min,MER}(\Delta T_{ref})} \tag{15}$$

Using the investment cost estimation for the heat exchangers of Chauvel et al. (2001), the bare module cost of the heat exchanger network $C_{BM,HEN}$ may be estimated by Equation 16. ΔT_{ref} is the decision variable to be optimised and represents the efficiency-investment trade-off in the heat exchanger network model. Considering the property of the exponential function used to calculate $C_{BM,HE}$, this approximation overestimates the real investment of a heat exchanger network with the same total area and the same number of exchangers (Ahmad et al., 1990).

$$\begin{aligned} C_{BM,HEN}(\Delta T_{ref}) &= \sum_{HE=1}^{n_{HE}} C_{BM,HE}(A_{HE}(\Delta T_{ref})) \\ &\approx N_{HE,min,MER} \cdot C_{BM,HE}(A_{mean}(\Delta T_{ref})) \end{aligned} \tag{16}$$

2.3 Process optimisation

2.3.1 Performance indicators

For energy conversion processes, key performance indicators typically address thermodynamic, economic and environmental performances of the process. They are computed using the thermo-economic model results and are often conflictive.

Highly integrated energy conversion processes often supply multiple services and require different energy inputs. Therefore, besides the energy efficiency ε, the exergy efficiency η is used to compare the work potential of the energy flows:

$$\varepsilon = \frac{\sum \Delta h_i^0 \dot{m}_i^- + \dot{Q}^- + \dot{W}^-}{\sum \Delta h_j^0 \dot{m}_j^+ + \dot{Q}^+ + \dot{W}^+} \tag{17}$$

$$\eta = \frac{\sum \Delta k_i^0 \dot{m}_i^- + \dot{E}_q^- + \dot{W}^-}{\sum \Delta k_j^0 \dot{m}_j^+ + \dot{E}_q^+ + \dot{W}^+} \tag{18}$$

In these definitions, Δh^0 and Δk^0 designate the lower heating and exergy values of products i and raw materials j, $\dot{Q}$ and $\dot{W}$ the useful heat and power and $\dot{E}_q$ the work potential of the heat. The superscripts '–' and '+' refer to produced (output) and consumed (input) services, respectively.$\dot{W}$ only occurs either in the numerator or denominator since the overall balance is of interest.

In addition to the grass roots cost C_{GR} that are calculated in the economic model, the assessment of plant economics requires an indicator for the working expenses. For this purpose, the plant's operating costs C_{OP} [€/MWh$_{SNG}$] are calculated considering the expenses for raw materials C_{RM}, utilities C_{UT}, operating labour C_{OL} and maintenance C_M, whereas the latter is supposed to amount to 5% of the investment per year:

$$C_{OP} = C_{RM} + C_{UT} + C_{OL} + C_M \tag{19}$$

with:

$$C_{RM} = \frac{\Delta h_{wood}^0 \dot{m}_{wood}}{\Delta h_{SNG}^0 \dot{m}_{SNG}} \cdot C_{wood} \tag{20}$$

$$C_{UT} = \frac{\dot{W}^+}{\Delta h_{SNG}^0 \dot{m}_{SNG}} \cdot C_{el} \tag{21}$$

$$C_{OL} = \frac{C_{salaries}}{P_a} \tag{22}$$

$$C_M = 0.05 \cdot \frac{C_{GR}}{P_a} \tag{23}$$

In this equations, C_{wood} and C_{el} correspond to the prices of wood and electricity, $C_{salaries}$ terms the employees' total yearly salaries and P_a the yearly production of SNG. By adding the discounted, annualised value of the initial investment divided by the yearly production P_a, the fixed and variable costs are combined to form the total production cost C_P [€/MWh$_{SNG}$]:

$$C_P = C_{OP} + \frac{(1+i_r)^n - 1}{i_r (1+i_r)^n} \cdot \frac{C_{GR}}{P_a} \tag{24}$$

where i_r is the interest rate and n the considered lifetime of the plant. This total production cost is expressed per unit of produced fuel and might be compared to fuel market prices to assess the profitability of the process.

The essential environmental goal of biofuel production is the mitigation of CO_2, whose effectiveness is conveniently summarised in terms of avoided CO_2 emissions. They are defined as the amount of CO_2 saved by substituting an equivalent fossil fuel with the produced synthetic fuel. As wood - and not SNG - thereby represents the limiting resource whose conversion into SNG is in competition with other applications, it is preferable to use the energetic value of wood and not SNG as functional unit.

Considering life cycle data of the material and energy streams, the avoided emissions $e_{a,wood}$ of using wood as SNG are expressed by the difference between the emissions for producing natural gas and SNG. The latter are thereby obtained by summing up the contributions of wood production, electricity production and the emissions at the plant:

$$e_{a,wood} = \frac{\Delta h^0_{SNG} \dot{m}_{SNG}}{\Delta h^0_{wood} \dot{m}_{wood}} \cdot e_{p,NG} - \left(e_{p,wood} + \frac{\dot{W}^+}{\Delta h^0_{wood} \dot{m}_{wood}} \cdot e_{p,el} + e_{plant} \right) \tag{25}$$

In this equation, $e_{a,i}$ terms the avoided emissions with respect to the use of substance i and $e_{p,i}$ to its production and transportation. In case of wood, $e_{p,wood}$ is negative since it includes its growth during which CO_2 is absorbed from the atmosphere. The emissions at the plant e_{plant} are assessed by an overall carbon balance of the plant and reported per MWh_{wood}:

$$e_{plant} = \frac{44/12 \cdot (\dot{m}_{C,wood} - \dot{m}_{C,SNG})}{\Delta h^0_{wood} \dot{m}_{wood}} \tag{26}$$

where $\dot{m}_{C,i}$ terms the partial mass flow of carbon and 44/12 is the ratio between the molecular mass of CO_2 and C.

2.3.2 Generation of optimal flowsheets using multi-objective optimisation

In order to identify best feasible solutions preserving the multiple aspects of the design problem, one of the key features of the approach is the use of a multi-objective optimisation strategy. This step can be seen as the generation of a set of optimal flowsheets for a specific production setting, i.e. the available feedstock type and size and the infrastructure of energy services. It allows engineers to compare "optimal" decisions, understand the compromise between conflicting objectives and analyse their impact on the decision variables.

The optimisation procedure aims at identifying a set of Pareto optimal process configurations in the search space, i.e. configurations for which it is not feasible to further decrease some objective without simultaneously increasing at least one other objective. Mathematically, these Pareto optimal process configurations x^* are defined by:

$$\begin{aligned} x^* \in P_k \quad \text{if} \quad & \nexists \ \{x \in S_k : (f_{\overline{o}}(x) < f_{\overline{o}}(x^*)) \wedge (f_o(x) \leq f_o(x^*))\} \\ & \forall \ \{\overline{o}, o \in O : \overline{o} \neq o\} \end{aligned} \tag{27}$$

where O, P_k and S_k represent the objective, Pareto and search space of a cluster k, respectively. The applied clustering techniques thereby preserve the diversity of the solutions by allowing suboptimal clusters to survive. This reveals to be important when it is desired to explore the entire search space and to identify break-even points of different technologies. Furthermore, the adopted algorithm developed by Leyland (2002) and Molyneaux (2002) iterates in an evolutionary procedure since the complicating decision variables (i.e. conversion pathways, equipment choices and process conditions) of the optimisation problem are of both integer and continuous type.

In principle, all the previously defined performance indicators are potential design targets, and the adopted algorithm is able to consider all of them as mathematical objectives. However, as the performance indicators f_i are different combinations of the underlying thermo-economic terms x_j (i.e. the utility and product streams and the total investment cost) and because this relation is similarly monotonic, i.e.:

$$f_i = f_i(x_j), \qquad \frac{\partial f_i}{\partial x_j} \text{ is of same sign } \forall f_i, x_j \tag{28}$$

these independent terms of the performance indicators are themselves used as objective functions. The condition of similar monotonicity thereby ensures that the Pareto set includes the optima not only for x_j, but all f_i. This approach reduces the number of objectives to a strict minimum and thus eases the interpretation of the numeric solutions. Moreover, it allows to generate a general set of optimal solutions

that is independent on arbitrarily chosen parameters like the interest rate, the specific emissions of the electricity mix, etc. (cf. Eqs 17 – 26) and guarantees to include the optima for any value of these parameters. Nevertheless, the assessment of the process performance with respect to the defined indicators is not omitted, but postponed to the results analysis that follows the generation of optimal solutions.

2.4 Results analysis and process synthesis

A detailed examination of the numerically generated set of optimal process configurations with regard to the multiple criteria will prepare the synthesis of a viable process. In addition to choosing an appropriate compromise, additional knowledge about the process is acquired and key issues of the process design and ongoing equipment development are determined. The analysis of the dependencies and trade-offs among the objectives and performance indicators is thereby extended with a statistical investigation of the decision variables' influence. In this work, we focus on analysing the search space through a histogram plot and characterising the relation between decision variables and objectives by Pearson's linear correlation coefficient ρ, defined as:

$$\rho_{i,j} = \frac{\mu(x_i - \mu(x_i))\mu(x_j - \mu(x_j))}{\sigma(x_i)\sigma(x_j)} \tag{29}$$

where μ and σ designate the mean and the variance of the observations x in the sets i and j. These coefficients provide a measure of how the observations of the sets are related: positive and negative values indicate directly and indirectly proportional relationships, values close to zero indicate that no correlation exists. In addition to ρ, partial correlation coefficients obtained from a multivariate regression are used to describe the same relation between two sets if all other decision variables are held fixed.

3 Example case: SNG from wood

Among the different biofuel production routes, thermochemical conversion of wood into methane is one of the most promising options with respect to environomic performance. The process considers a potentially abundant feedstock which is not in competition with food production and also includes wastes. Being the main constituent of natural gas, existing infrastructure can be used to distribute a renewable fuel of high quality for transport applications and cogeneration. The process itself is energy efficient and economically viable already at small scales and therefore well suited for local feedstocks that are typical for biomass.

3.1 Block flow superstructure

The most common route for the thermochemical conversion of wood into SNG is gasifying the feedstock in the absence of nitrogen, converting the cleaned producer gas into methane and separating the remaining carbon dioxide from the product gas to meet a Wobbe index between 13.3 and 15.7 kWh·Nm^{-3} (TISG, 2000). Alternatively to separate gasification and methanation, Waldner and Vogel (2005) demonstrated at lab scale that catalytic hydrothermal gasification in supercritical water would allow for direct and complete conversion of the feedstock into methane. Since high humidity content in the feedstock deteriorates the gasifier performance, a drying stage is normally considered in the feed preparation. Using the carbon atom as reference to represent dry wood as a molecule, the thermochemical conversion is conveniently represented with the stoichiometry of Equation 30:

$$CH_{1.35}O_{0.63} + 0.3475\, H_2O \overset{\Delta H^0 = -10.5 kJ \cdot mol^{-1}_{wood}}{\rightarrow} 0.51125\, CH_4 + 0.48875\, CO_2 \tag{30}$$

A process block flow diagram assembling the technology for the classical wood to SNG route with separate gasification and methanation is given in Figure 2. The highlighted pathway thereby indicates the exemplary configuration that is examined here to illustrate the design approach. It considers a drying

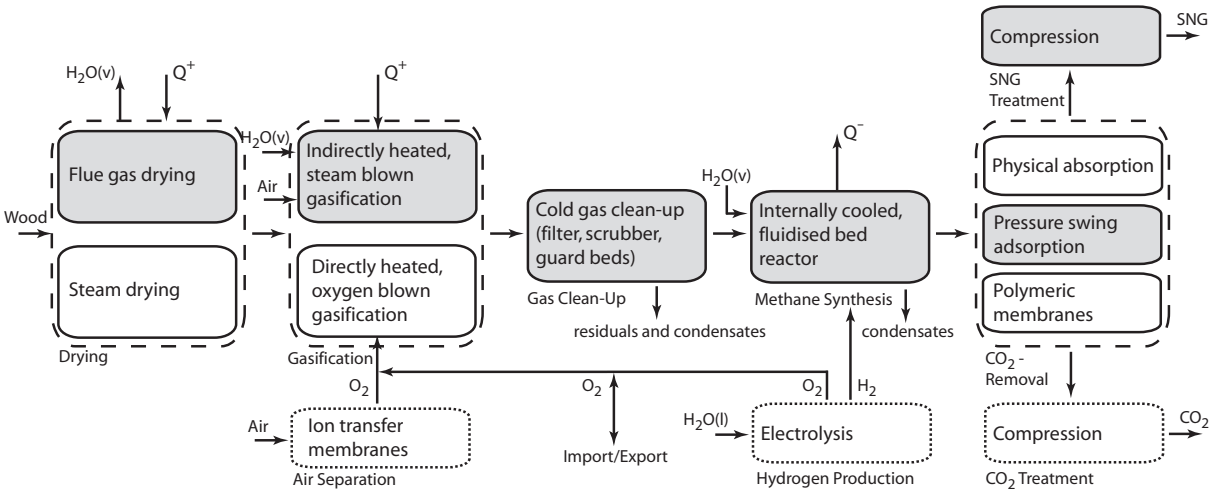

Figure 2: Process superstructure. Dashed boxes assemble competing technologies and dotted ones are used for optional equipment. The examined process configuration is shown shaded.

stage with hot air followed by indirectly heated, fluidised bed gasification with a separate combustion chamber that supplies the heat through recirculation of hot bed material (Hofbauer et al., 2002). A conventional, cold gas clean-up and compression stage prepares the producer gas for methane synthesis in an internally cooled, pressurised catalytic fluidised bed reactor. Carbon dioxide is removed from the product stream in a pressure swing adsorption system with four adsorption vessels. Its energy density is thus adjusted according to the specifications of the gas grid, on which the SNG is injected at a pressure of 50 bar. An overview of the nominal operating conditions and its feasible range is given in Table 1.

3.2 Thermo-economic model

In previous work, the energy-flow and energy-integration models have been developed and approximate sizing and cost estimations have been done (Duret et al., 2005; Gassner and Maréchal, 2005, 2008). The energy-flow of the reactor sections are thereby modelled using equilibrium relationships. Whereas the equilibrium assumption holds for methane synthesis in a catalytic fluidised bed, gasification reactors do generally not reach equilibrium. Artificial temperature differences are therefore introduced as parameters in the calculation of the equilibrium constant to fit the data according to the composition of the producer gas observed in pilot plants. Contrary to the conventional simulation approach applied by Schuster et al. (2001) for indirectly heated gasification, the energy-flow model only deals with the actual transformation (i.e. the gasification, depicted on the right side of Figure 3) and determines its heat demand. The technological implementation to satisfy this demand (i.e. combustion of residual char and cold producer

Table 1: Nominal operating conditions of the process and feasible range for optimisation.

Section	Operating conditions		Unit	Nominal	Range
Drying	Inlet temperature	$T_{d,in}$	K	473	[433; 513]
	Outlet wood humidity	$\Phi_{w,out}$	%wt	20	[5; 35]
Gasification	Pressure	p_g	bar	1	-
	Gasification temperature	T_g	K	1123	[1073; 1173]
	Steam preheat temperature	$T_{g,p}$	K	673	[573; 873]
	Steam to dry biomass ratio	$r_{S/B}$	%wt	50	-
Methanation	Pressure	p_m	bar	15	[1; 50]
	Inlet temperature	$T_{m,in}$	K	673	[573; 673]
	Outlet temperature	$T_{m,out}$	K	673	[573; 673]
CO_2-removal	Adsorption pressure	p_a	bar	5.5	-

Table 2: Nominal operating conditions of the Rankine cycle and feasible range for optimisation.

Operating conditions		Unit	Nominal	Range
Production pressure	$p_{s,p}$	bar	60	[40; 100]
Superheat temperature	$T_{s,s}$	K	773	[623; 823]
1^{st} utilisation level	$T_{s,u1}$	K	465	-
2^{nd} utilisation level	$T_{s,u2}$	K	423	[323; 523]
condenser inlet	$T_{s,c,in}$	K	293	-
condenser outlet	$T_{s,c,out}$	K	291	-

gas in an attached reactor and heat transfer by recirculation of hot bed material) is not imposed, but the heat requirement itself is transferred to the energy-integration model. Instead of fixing one specific stream (i.e. cold producer gas in the case of Schuster et al.) as fuel for the gasifier, the optimal choice and amount of the streams used as fuel will be determined by the energy integration of the whole system. In the examined process configuration, unconverted char and gaseous residue of the condensates from methane synthesis are considered as waste streams to be burnt. Additional streams for fuel supply are chosen among the hot and cold producer gas from the gasifier and the gas cleaning outlets instead of only considering the cold producer gas as fuel.

As indicated by Equation 30, the overall reaction is exothermal and thermal energy must be withdrawn from the the process. Since the process pinch is generally located at the gasification temperature, the excess heat is available at high temperature and allows for the cogeneration of electricity in a Rankine cycle. For conceptual design purposes, a simple cycle layout with one production, two usage and one condensation level with the parameters given in Table 2 are thereby considered.

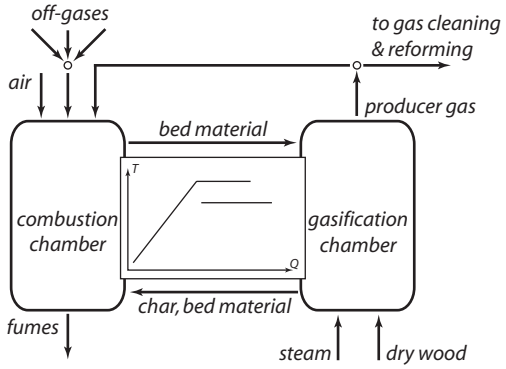

Figure 3: Decomposed thermodynamic model of an indirectly heated gasifier.

3.3 Generation of optimal flowsheets using multi-objective optimisation

For the design example of this paper, the plant is supposed to be connected to the gas and electricity grids. This allows for gas production and power recovery from excess heat by means of a Rankine cycle, whereas no external heat sources or heat marketing opportunities are available. The capacity of the plant is fixed to 20 MW_{th} based on the lower heating value of wood with the properties given in Table 3. Table 4 shows the considered conditions for the economic evaluation. Consistently with the performance indicator definition, three objectives are used in the optimisation problem, i.e. the plant's SNG output ($\Delta h^0_{SNG}\dot{m}^-_{SNG}$), its electricity generation (W^-) and its grass roots cost (C_{GR}). The energy integration is accomplished by maximising the fuel production. The decision variables and their domain have already been identified in the elaboration of the process superstructure and are shown in Tables 1 and 2.

Table 3: Proximate and ultimate analysis of wood.

Proximate analysis			Ultimate analysis					
Δh^0_{wood} [a]	16.2	MJ/kg$_{dry}$	C	51.09	%wt	O	42.97	%wt
Δk^0_{wood} [b]	20.9	MJ/kg$_{dry}$	H	5.75	%wt	N	0.19	%wt
Moisture	50.0	%wt						

[a] Δh^0_{wood} is calculated considering the latent heat of vaporisation for moisture and referred to the dry mass of wood, i.e. $\Delta h^0_{wood} = \Delta h^0_{wood,dry} - \Delta h_{vap}\Phi_w/(1-\Phi_w)$.

[b] Chemical exergy is calculated according to Szargut and Styrylska (1964).

Table 4: Assumptions for the economic analysis.

Parameter	Value	Parameter	Value
Marshall&Swift index (2004)	1197	Operators[a]	4 p./shift
Dollar exchange rate	1 €/US$	Operator salary	60 k€/year
Interest rate	6%	Wood price (Φ_w=50%wt)	16.7 €/MWh
Expected lifetime	15 years	Electricity price (import)	88.9 €/MWh
Plant availability	90%	Electricity price (export)	26.4 €/MWh
Maintenance costs	5%/year of C_{GR}		

[a] Full time operation requires three shifts per day. With a working time of five days per week and 48 weeks per year, one operator per shift corresponds to 4.56 employees.

3.4 Results analysis

The plots of Figure 4 show the numeric results from the process optimisation in the objective space. As the optimal set is generated with respect to three objectives, the Pareto front, i.e. the optimal trade-off between the objectives, is expected to be three-dimensional. Its two-dimensional projection is thus scattered and optimal points of the third objective appear in the suboptimal domain of the other two. Nevertheless, the plot clearly shows the trade-off between gas and electricity generation. Due to the energy conservation principle, these terms are conflictive and an increase in SNG production increases the need for electricity. It is thereby interesting that – dependent on the chosen configuration – the plant might consume or generate power, and the best set-up will heavily depend on the cost of buying or selling electricity.

To analyse the importance of the output streams, Figure 5 shows the energetic, economic and environmental performance indicators with respect to these two objectives. Table 5 reports the decision

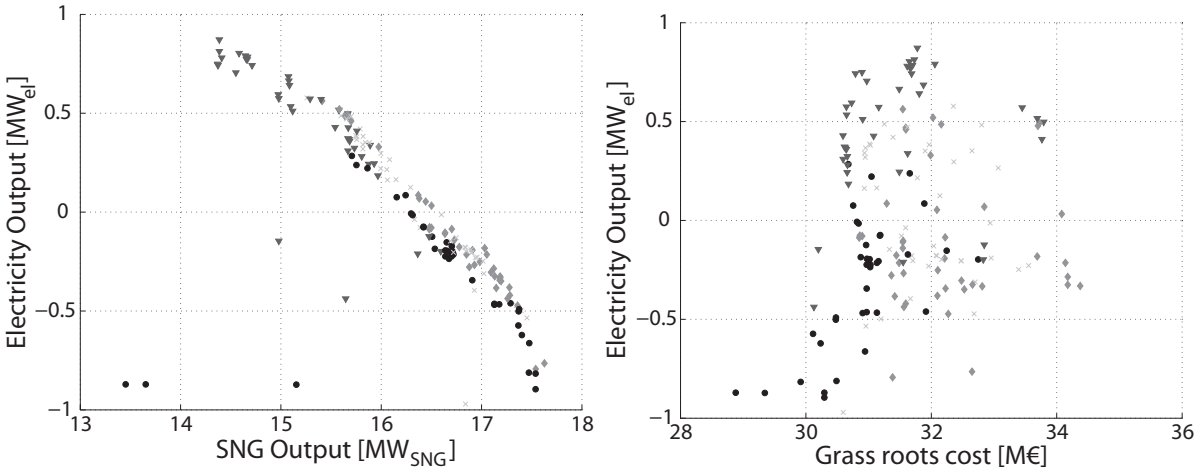

Figure 4: Optimal solutions in the Pareto domain. Marker symbols indicate cluster affiliations.

variables, the objectives and the performance indicators for some plant configurations that are optimal with respect to the individual objectives and performance indicators. From an energy conversion point of view, a high gas output is clearly preferable. With increasing production of SNG, the energy and exergy efficiencies reach up to 85% and 69% respectively. The considerable benefit of high conversion efficiencies at high gas output rates further effects on the economic performance. Despite the elevated marginal efficiency for electricity generation $\delta W^{-}/\delta(\Delta h^{0}_{SNG}\dot{m}_{SNG})$ of about 50%, the relatively low benefit from selling electricity at 26.4 €/MWh$_{el}$ inhibits solutions with net power production to pay off. If only operating costs are considered, the economic performance indicators suggest a robust plant design with a neutral power balance, although some more profit over the considered lifespan is obtainable with a cheaper, but slightly more power-consuming process. According to the Table, good solutions result in operating and production costs around 42 and 65 €/MWh$_{SNG}$, respectively. Independent on the chosen configuration, the environmental balance in terms of avoided CO_2 emissions is truly positive. Allocating fossil emissions of 230 kg$_{CO2}$/MWh$_{NG}$ to the use of natural gas, up to 192 kg$_{CO2}$/MWh$_{wood}$ (= 218 kg$_{CO2}$/MWh$_{SNG}$) are avoided by substitution, if the CO_2 emissions from the plant are not sequestrated. Its sequestration at the process outlet would allow to turn the process into an overall CO_2 sink. For maximum gas output, potentially 350 kg$_{CO2}$/MWh$_{wood}$ (= 397 kg$_{CO2}$/MWh$_{SNG}$) of fossil emissions are avoided, which corresponds to the absorption of 147 kg$_{CO2}$/MWh$_{wood}$ (= 167 kg$_{CO2}$/MWh$_{SNG}$) from the atmosphere.

Figures 6 and 7 allow to analyse the relation between the decision variables and the performance of the plant. The correlation coefficients between variables and objectives indicate the key parameters that essentially determine the plant characteristics. Especially for the wood humidity after drying $\Phi_{w,out}$ and the gasification temperature T_g, both the linear and partial linear correlation coefficients with the SNG and electricity generation are significant. The comparably high absolute value of the total correlation coefficient of the gasification steam preheat temperature $T_{g,p}$ further suggest an interaction between these parameters, which is explained by the energy integration of the process. Since gasification is endothermal and requires heat at the highest temperature level, its demand determines the pinch point of the process streams shown on Figure 8. Both wood moisture and steam are cold streams that are injected into the gasifier at a temperature well below the pinch point. For their evaporation and superheating to the vessel temperature, they consume an important amount of heat from the hot utility transferred through the pinch. As the energy requirement at high temperature is satisfied by combustion of some of the produced gas, high moisture content and low steam preheat temperature directly decrease the SNG output. In the heat cascade, their latent heat is added at the pinch and partly recovered by the Rankine cycle to produce power. With increasing gasification and pinch point temperature, this effect occurs even more remarked. The correlation coefficients between the variables and the capital cost are less significant. Solely the pressure of the methane synthesis reactor p_m seems to remarkably influence the total system cost, which is due to a smaller and less costly reactor for increasing pressure.

Although the correlation coefficients allow for analysing the interdependencies between decision variables and objectives in the Pareto set, they do not give any indication about the absolute position and distribution of the optimal values of the variables in the search space. For this purpose, a histogram of their observations in the Pareto set is shown on Figure 7. In addition to the number of observations given by the bar width, the shading of the bars relate to the ranking of the points with respect to one of the objectives. If the points in the set rank inversely with respect to the objectives (which occurs in a well developed, two-dimensional optimisation) the shading of the bars is inverse and one plot is sufficient to represent the ranking with regard to both objectives. Although this is not the case in the design example, only one exemplary set of histograms ranked with respect to the SNG output is shown for simplicity. In addition to the significant correlations of wood humidity, gasification temperature and preheat temperature, the plots show that some variables are fairly uniformly distributed in the search space (e.g. $\Phi_{w,out}$, $T_{m,in}$, $p_{s,p}$), some concentrate in a restricted domain inside the interval (p_m, $T_{s,u2}$) and some clearly approach a bound (T_g and the integer decision variable for using a Rankine cycle). These types indicate genuine design choices, less conflicting parameters and technological limits that inhibit better performance with respect to all objectives.

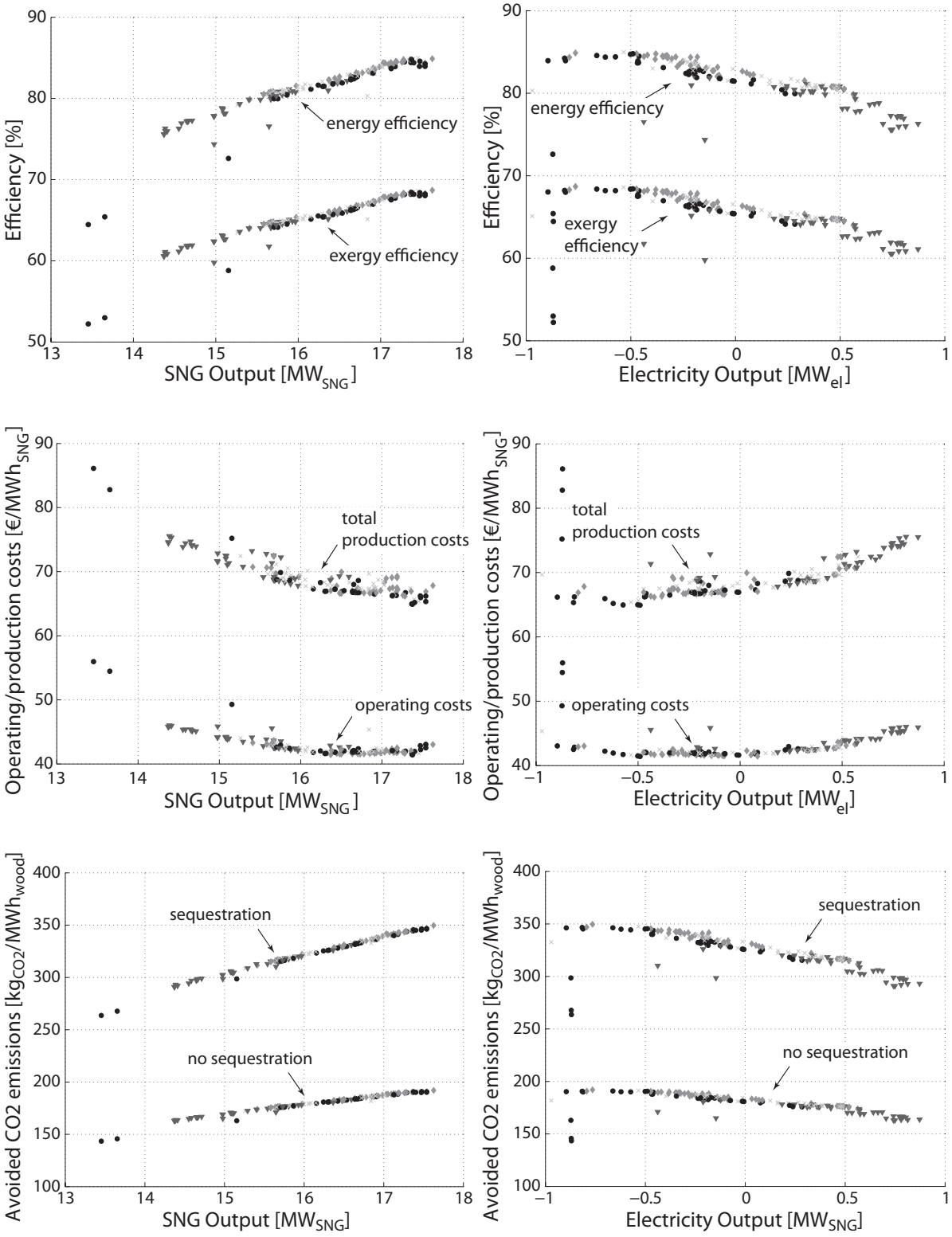

Figure 5: Performance indicators for the set of generated flowsheets. Marker symbols indicate cluster affiliations.

Table 5: Decision variables, objectives and performance indicators of some selected process designs.

	Unit	$C_{GR,min}$	W^-_{max}	$W^- \approx 0$	$C_{P,min}$[a]	ε_{max}	η_{max}[b]
$T_{d,in}$	K	509	507	501	507	507	506
$\Phi_{w,out}$	%wt	18.9	32.4	25.1	9.72	9.58	5.38
T_g	K	1115	1132	1075	1074	1073	1075
$T_{g,p}$	K	851	699	815	816	843	837
p_m	bar	6.84	5.18	12.3	8.44	9.70	5.49
$T_{m,in}$	K	586	663	608	606	652	658
$T_{m,out}$	K	588	589	580	584	620	583
$p_{s,p}$	K	48.7	53.9	64.6	78.3	72.6	73.3
$T_{s,s}$	K	745	816	792	764	820	754
$T_{s,u2}$	bar	377	404	430	411	411	407
$\Delta h^0_{SNG}\dot{m}^-_{SNG}$	MW	13.7	14.4	16.3	17.4	17.5	17.6
W^-	MW	-0.87	0.87	-0.01	-0.49	-0.53	-0.76
C_{GR}	M€	28.9	31.8	30.8	30.4	31.0	32.7
ε	%	65.4	76.3	81.5	84.8	85.0	84.9
η	%	53.0	61.1	65.4	68.4	68.6	68.7
C_{OP}	€/MWh$_{SNG}$	54.5	45.9	41.6	41.4	41.6	43.0
C_P	€/MWh$_{SNG}$	82.8	75.5	66.9	64.9	65.4	67.8
$e_{a,wood,no\ seq.}$	kg$_{CO2}$/MWh$_{wood}$	146	164	181	191	191	192
$e_{a,wood,seq.}$	kg$_{CO2}$/MWh$_{wood}$	268	293	326	345	347	350

[a] corresponds also to minimum C_{OP}

[b] corresponds also to maximum $\Delta h^0_{SNG}\dot{m}^-_{SNG}$ and maximum $e_{a,wood}$

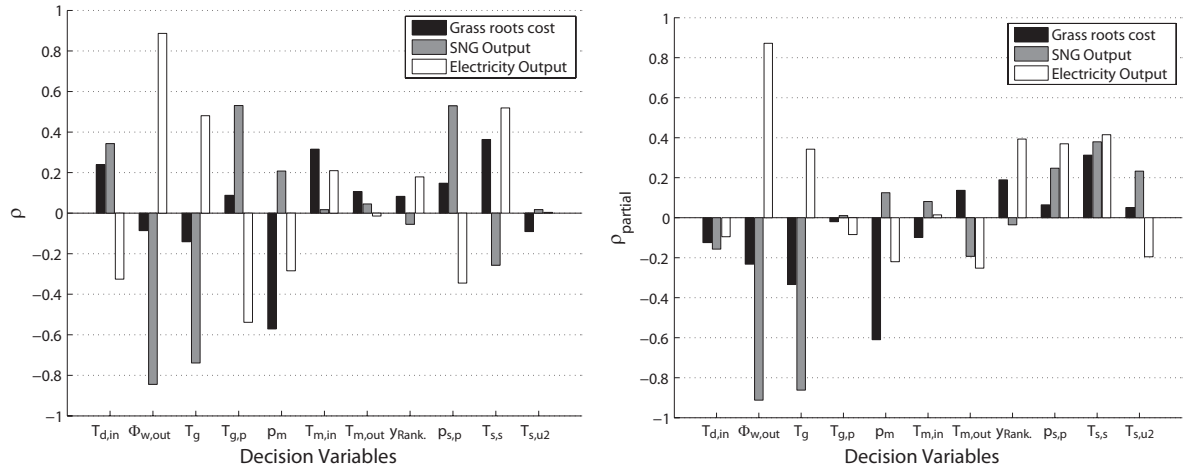

Figure 6: Linear (left) and partial linear correlation coefficient between variables and objectives.

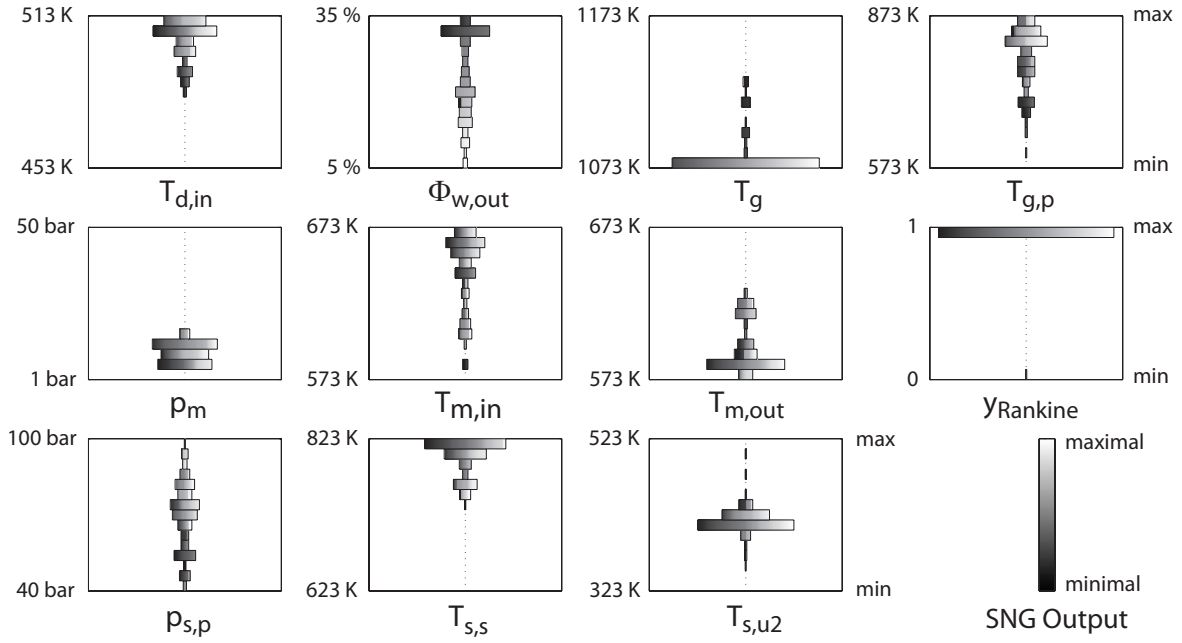

Figure 7: Variable distribution in search space ranked with respect to SNG output.

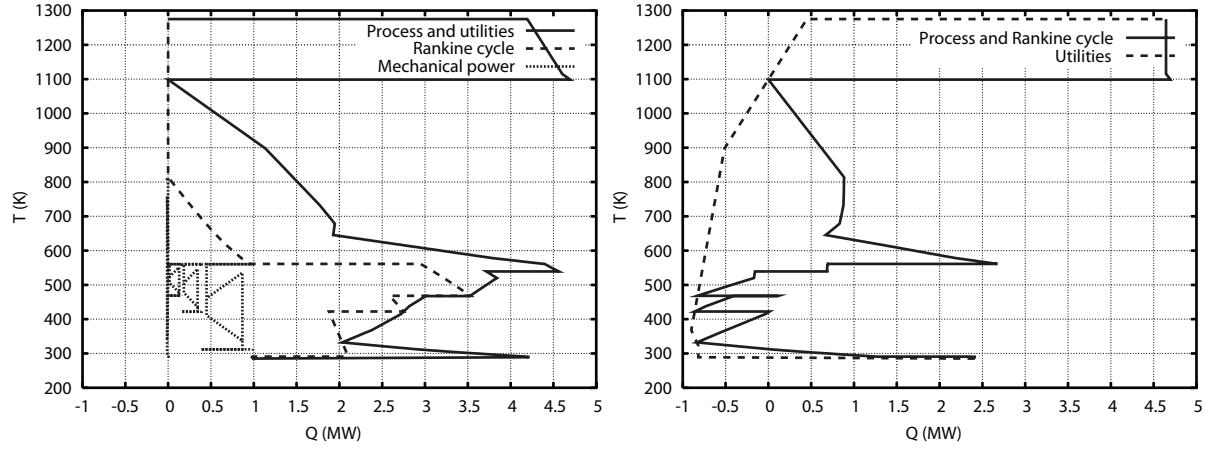

Figure 8: Integrated composite curves of a solution with neutral overall power balance.

4 Conclusions

Due to the separate modelling of the thermodynamic conversions and their thermal integration, the methodology presented here avoids to restrict the investigated process layouts to a very limited number of scenarios at an early stage of the design. Instead, its coupling with cost estimation procedures that consider the thermodynamic conditions and the usage of a multi-objective optimisation algorithm allows to systematically generate a set of best flowsheets for a given production setting. The methodology is thus very suitable for the conceptual design of integrated biofuel plants. It should be understood as a tool that efficiently eliminates solutions that are not worth investigating in detail, identifies the most promising process layouts and operating conditions, targets ideal performance and guides the efforts in R&D towards potentially optimal plants.

References

Ahmad, S., Linnhoff, B., Smith, R., 1990. Cost optimum heat exchanger networks - 2. targets and design for detailed capital cost models. Computers and chemical engineering 14 (7), 757–767.

Belsim SA, 2007. Vali IV.
URL `http://www.belsim.com`

Bolliger, R., Favrat, D., Maréchal, F., 2005. Advanced power plant design methodology using process integration and multi-objective thermo-economic optimisation. In: Proceedings of the 18th International conference on efficiency, cost, optimization, simulation and environmental impact of energy systems (ECOS).

Chauvel, A., Fournier, G., Raimbault, C., 2001. Manuel d'évaluation économique des procédés. Technip, Paris.

Douglas, J. M., 1985. Hierarchical decision procedure for process synthesis. AIChE Journal 31, 353–362.

Douglas, J. M., 1988. Conceptual design of chemical processes. McGraw-Hill, New York.

Duret, A., Friedli, C., Maréchal, F., 2005. Process design of Synthetic Natural Gas (SNG) production using wood gasification. Journal of cleaner production 13, 1434–1446.

Floudas, C., Ciric, A., Grossmann, I., 1986. Automatic synthesis of optimum heat exchanger network configurations. AIChE Journal 32 (2), 276–290.

Gassner, M., Maréchal, F., 2005. Thermo-economic model of a process converting wood to methane. Submitted to Biomass and bioenergy.

Gassner, M., Maréchal, F., 2008. Thermo-economic optimisation of the integration of electrolysis in synthetical natural gas production from wood. Energy 33, 189–198.

Hamelinck, C. N., Faaij, A. P. C., den Uil, H., Boerrigter, H., 2004. Production of FT transportation fuels from biomass; technical options, process analysis and optimisation, and development potential. Energy 29, 1743–1771.

Hofbauer, H., Rauch, R., Löeffler, G., Kaiser, S., Fercher, E., Tremmel, H., 2002. Six years experience with the FICFB-gasification process. In: Proceedings of the 12th European conference and technology exhibition on biomass for energy, industry and climate protection. Amsterdam, Netherlands.

Kravanja, Z., Glavic, P., 1997. Cost targeting for HEN through simultaneous optimization approach: a unified pinch technology and mathematical programming design of large HEN. Computers and chemical engineering 21 (8), 833–853.

Leyland, G. B., 2002. Multi-objective optimisation applied to industrial energy problems. Ph.D. thesis, Ecole polytechnique fédérale de Lausanne.

Maréchal, F., Kalitventzeff, B., 1998. Process integration: Selection of the optimal utility system. Computers and chemical engineering 22, S149–S156.

Molyneaux, A., 2002. A practical evolutionary method for the multi-objective optimisation of complex integrated energy systems including vehicle drivetrains. Ph.D. thesis, Ecole polytechnique fédérale de Lausanne.

Mozaffarian, M., Zwart, R. W. R., 2003. Feasibility of biomass/waste-related SNG production technologies. Tech. rep., ECN, Petten.

Palazzi, F., Maréchal, F., van Herle, J., Autissier, N., 2005. A methodology for thermo-economic modeling and optimization of SOFC systems. Chemical engineering transactions 7, 13–18.

Schuster, G., Löffler, G., Weigl, K., Hofbauer, H., 2001. Biomass steam gasification - an extensive parametric modeling study. Bioresorce technology 77, 71–79.

Szargut, J., Styrylska, T., 1964. Angenäherte Bestimmung der Exergie von Brennstoffen. Brennstoff-Wärme-Kraft 16 (12), 589–636.

Tijmensen, J. A. M., Faaij, A. P. C., Hamelinck, C. N., van Hardeveld, M. R. M., 2002. Exploration of the possibilities for production of Fischer Tropsch liquids and power via biomass gasification. Biomass and Bioenergy 23, 129–152.

TISG, 2000. Einspeisung von Klärgas ins öffentliche Erdgas-Verteilnetz. Merkblatt 013/d. Zürich.

Turton, R., Bailie, R. C., Whiting, W. B., Shaeiwitz, J. A., 1998. Analysis, synthesis, and design of chemical processes. Prentice Hall, New York.

Ulrich, G.-D., 1984. A guide to chemical engineering process design and economics. Wiley, New York.

Waldner, M. H., Vogel, F., 2005. Renewable production of methane from woody biomass by catalytic hydrothermal gasification. Industrial and Engineering Chemistry Research 44, 4543–4551.

Zwart, R. W. R., Boerrigter, H., 2005. High efficiency co-production of Synthetic Natural Gas (SNG) and Fischer-Tropsch (FT) transportation fuels from biomass. Energy and Fuels 19, 591–597.